

Spin Dynamics in an Ordered Stripe Phase

J. M. Tranquada,¹ P. Wochner,¹ and D. J. Buttrey²

¹*Physics Department, Brookhaven National Laboratory, Upton, New York 11973*

²*Department of Chemical Engineering, University of Delaware, Newark, Delaware 19716*

(December 2, 1996)

Inelastic neutron scattering has been used to measure the low-energy spin excitations in the ordered charge-stripe phase of $\text{La}_2\text{NiO}_{4+\delta}$ with $\delta = 0.133$. Spin-wave-like excitations disperse away from the incommensurate magnetic superlattice points with a velocity $\sim 60\%$ of that in the $\delta = 0$ compound. Incommensurate inelastic peaks remain well-resolved up to at least twice the magnetic ordering temperature. Paramagnetic scattering from a $\delta = 0.105$ sample, which has a Néel-ordered ground state, shows anomalies suggestive of incipient stripe correlations. Similarities between these results and measurements on superconducting cuprates are discussed.

75.30.Ds, 75.30.Fv, 71.45.Lr, 74.72.-h

Hole-doped La_2NiO_4 is a strongly-correlated electron system that exhibits an exotic form of charge order. Although many questions concerning this order remain to be answered, the basic nature of the charge and associated spin order has now been fairly well established by scattering studies [1,2,3,4,5,6]. At sufficiently high levels of doping ($\gtrsim 0.15$ holes/Ni), the added holes, which enter the NiO_2 planes, order in periodically spaced stripes. The Ni spins in the intervening regions order antiferromagnetically, with an antiphase relationship between neighboring domains. To make further progress toward understanding the spatially-inhomogeneous charge and spin correlations in this system, it is necessary to study the spin and charge dynamics. Some information on charge dynamics has been provided by infrared reflectivity studies [7]. Here we present an inelastic neutron scattering study that compares the spin dynamics in 3 distinct phases of $\text{La}_2\text{NiO}_{4+\delta}$, one with a stripe-ordered ground state ($\delta = 0.133$) and two with Néel-ordered ground states ($\delta = 0$ and 0.105).

Static stripe order has also been observed in the cuprate system $\text{La}_{1.6-x}\text{Nd}_{0.4}\text{Sr}_x\text{CuO}_4$ [8], where it has been shown to coexist with superconductivity [9]. The \mathbf{Q} dependence of the magnetic scattering is essentially identical with that of the dynamical spin correlations found in $\text{La}_{2-x}\text{Sr}_x\text{CuO}_4$ [10]. Given the empirical similarities between stripe-ordered phases in the nickelates and cuprates, it is essential to explore similarities and differences of the spin dynamics in these two classes. Such comparisons are made throughout the paper.

Some characterization of spin excitations associated with stripe order was reported by Hayden *et al.* [1] in their pioneering study of incommensurate magnetic correlations in a sample of Sr-doped La_2NiO_4 ; however, the short spin-spin correlation length associated with the dilute and randomly distributed dopants limited the information that could be obtained. Oxygen-doped samples have the advantage that for $\delta \gtrsim 0.11$, the interstitials

and the charge stripes both order 3-dimensionally [3,4,5]. Previous neutron-scattering studies of spin dynamics in $\text{La}_2\text{NiO}_{4+\delta}$ [11,12,13,14] have focussed on samples with δ in the range $0 \leq \delta \lesssim 0.11$, throughout which the magnetic order remains commensurate, albeit with a strong variation in ordering temperature, T_N [15,16]. The reduction in T_N with increasing δ is accompanied by a dramatic decrease in the spin-wave velocity, the change being a factor of ~ 3 between $\delta = 0$ and 0.077 [11,12,13]. Above T_N , the instantaneous magnetic correlation length is found to decay with temperature much more rapidly at higher δ [14].

A simple extrapolation of the lower δ results might lead one to expect that an increasing hole density would result in a severe reduction in the effective magnetic interaction strength. To the contrary, we will demonstrate that at higher δ , where the holes order in charge stripes, the spin waves, dispersing away from incommensurate wave vectors, actually harden. The incommensurability of the low-energy spin fluctuations remains well resolved up to at least twice the magnetic ordering transition, T_m . Furthermore, we will show that, despite commensurate order below ~ 50 K, the paramagnetic scattering from a $\delta = 0.105$ crystal is inconsistent with the behavior expected for a quasi-2D Heisenberg system such as La_2NiO_4 [17]. The development of a temperature- and energy-independent lineshape for $T \gtrsim 120$ K is suggestive of incipient charge-stripe correlations.

The crystals of $\text{La}_2\text{NiO}_{4+\delta}$ with $\delta = 0, 0.105$, and 0.133 discussed here have been characterized elsewhere [5,16]. The interstitials in the $\delta = 0.105$ sample (and throughout the range $0.05 \lesssim \delta \lesssim 0.11$) exhibit a 1-dimensional staging order [16], whereas those in the $\delta = 0.133$ sample order 3-dimensionally [5]. The change in the nature of the interstitial order is correlated with the change in character of the spin and charge order.

Inelastic neutron scattering measurements were performed on triple-axis spectrometers at Brookhaven Na-

tional Laboratory's High Flux Beam Reactor. Neutrons were monochromatized and analyzed with pyrolytic graphite (PG) crystals set for the (002) reflection. The final neutron energy was fixed at 14.7 meV, and a PG filter was used to eliminate higher order neutrons from the scattered beam. Coarse horizontal collimations were selected (40'-40'-80'-80' for most of the measurements). Each sample was cooled with a Displex closed-cycle He refrigerator.

To describe the results we will make use of a unit cell of size $\sqrt{2}\mathbf{a}_t \times \sqrt{2}\mathbf{a}_t \times \mathbf{c}_t$ relative to the simple tetragonal one. The antiferromagnetic wave vector for a single NiO₂ layer is then (1, 0, 0), or equivalently (0, 1, 0), where reciprocal lattice vectors \mathbf{Q} are specified in units of $(\frac{2\pi}{a}, \frac{2\pi}{a}, \frac{2\pi}{c})$. The spin fluctuations in the stripe-phase sample were measured in the $(h, k, 0)$ zone near (0, 1, 0). To simplify comparison, the dispersion results for the Néel-ordered samples will also be presented in the $(h, k, 0)$ zone, although they were actually measured in a different zone.

To optimize the resolution and cross section, spin-wave measurements of the $\delta = 0$ and $\delta = 0.105$ samples were performed in the $(h, 0, l)$ zone, either by scanning h at fixed energy transfer or by scanning the energy transfer at fixed h , with l selected to minimize the effective resolution width. The results obtained at low temperature (~ 10 K) are indicated by the circles ($\delta = 0$) and triangles ($\delta = 0.105$) in Fig. 1. The lines through the data are spin-wave dispersion curves with the spin-wave velocities, $\hbar c$, as shown in Table I. The velocity for $\delta = 0$ is taken from Ref. [12], whereas that for the 0.105 sample is a fit to the data. The two curves for each δ correspond to in-plane and out-of-plane spin-wave modes, which have different anisotropy gaps as discussed in Ref. [13]. On increasing δ from 0 to 0.105, we find a decrease of the spin-wave velocity by a factor of 5, consistent with, though more extreme than, the earlier results [11].

This trend is abruptly reversed on entering the stripe-ordered phase found at $\delta = 0.133$. The measurements on this sample were performed in the $(h, k, 0)$ zone, with constant-energy scans through the incommensurate peak at $(\epsilon, 1, 0)$. Scans were taken both along $(h, 1, 0)$, in the direction of the modulation, and along $(\epsilon, k, 0)$, parallel to the stripes. These scan directions are indicated in the left inset of Fig. 1 as *A* and *B*, respectively. The data collected at 80 K are shown in Fig. 2, with the intensity multiplied by the energy transfer, $\hbar\omega$, to compensate for the spin-wave-like fall off of intensity with energy. If the excitations truly are like spin waves, then we would expect to see two peaks dispersing away from the incommensurate wave vector as $\hbar\omega$ increases. The scans along *B* in Fig. 2(b) appear consistent with such a model, and the two peaks are almost resolved at $\hbar\omega = 8$ meV. The peak separations obtained by fitting symmetric pairs of Gaussian peaks to the data are shown in the right inset of Fig. 1, and the resulting spin-wave velocity is listed in Table I. In contrast, the scans along *A* in Fig. 2(a) show a

single broad peak at each energy, with the width increasing linearly with energy. (Resolution does not limit the width except possibly at 2 meV.) The results of Gaussian fits are shown in Fig. 1.

Looking at Table I, we see that the spin-wave velocity for excitations propagating parallel to the stripes is $\sim 60\%$ of that in the $\delta = 0$ sample, and 3 times greater than the velocity for $\delta = 0.105$. The decrease relative to $\delta = 0$ reflects the weakened exchange between spins separated by a charge stripe. In a simple Heisenberg antiferromagnet, $\hbar c$ is proportional to the product of the superexchange energy J and the number of nearest neighbors. A large part of the decrease in $\hbar c$ can be attributed to the effective reduction in the number of nearest neighbors. In contrast, excitations perpendicular to the stripes appear to have a greater damping, perhaps due to a more direct coupling to the dynamical spin degrees of freedom associated with the charge stripes.

We have also measured spin excitations in the charge-ordered, paramagnetic phase of the $\delta = 0.133$ sample at $T > T_m = 110.5$ K. Figure 3 shows scans along the modulation direction at $\hbar\omega = 4$ meV for three different temperatures. Although the peak widths increase with temperature, the incommensurate peaks remain well resolved even at $T = 2T_m$. The charge order is finite but extremely weak at this point [5].

How do the above results relate to La_{2-x}Sr_xCuO₄? In the cuprate it has been shown that the scattering from low-energy spin excitations peak at incommensurate positions, with the peak widths increasing with both energy and temperature [10]. An explanation of how the incommensurability can be understood in terms of stripe correlations has been given elsewhere [8]. The present results demonstrate that the spin excitations in a stripe-ordered nickelate phase exhibit an energy dispersion and thermal broadening that is qualitatively similar to that found in the cuprate system. Such an interpretation is also consistent with the recent finding that the high-energy spin excitations in La_{1.86}Sr_{0.14}CuO₄ have a spin-wave-like character [18]. Of course, there is no static order of stripes in the cuprates with optimal superconductivity—the dynamic nature of the stripes is presumably related to the more quantum mechanical nature of the cuprates. Nevertheless, it has been shown elsewhere [9] that superconductivity can coexist with stripe order.

Now let us return to the $\delta = 0.105$ sample. Remember that the Ni moments order commensurately below ~ 50 K, and that the spin waves found at low temperature are strongly renormalized by the doped holes. If we look at $T > T_N$, the spin waves are overdamped, and a constant-energy scan through \mathbf{Q}_{AF} yields a single, broad peak. The peak widths as a function of temperature for 3 different energies are indicated on the right-hand side of Fig. 4. Initially, the peak widths increase with energy, as well as temperature, but for $T \gtrsim 120$ K the widths become independent of energy and temperature. Fur-

thermore, as indicated on the left side of Fig. 4, the peak shape is rather flat topped.

The energy-independence suggests that the peak shape is determined predominantly by a modulation of the dynamical spin correlations in real space. In fact, we can describe the peak shape quite well with a simple model of antiphase AF domains with correlations between domains that decay exponentially with distance. If we consider domains of width $2a$ (4 Ni spins wide along [010]) as observed in a Sr-doped sample with comparable hole density [6], then the scattered intensity along $(0, k, 0)$ should have the form

$$I = AF^2 \frac{1 - p^2}{1 + p^2 + 2p \cos(4\pi k)}, \quad (1)$$

where A is a scale factor, $p = e^{-2a/\xi}$ with ξ being the correlation length, and

$$F = 2 \left[\sin\left(\frac{1}{2}\pi k\right) - \sin\left(\frac{3}{2}\pi k\right) \right]. \quad (2)$$

We get an excellent fit to the data, shown by the curves in Fig. 4, if we set $p = 0.1$, corresponding to $\xi = 0.87a = 4.7 \text{ \AA}$. The weakly correlated antiphase magnetic domains imply charge segregation. The disappearance of these incipient stripe correlations at low temperature contrasts with the case of $\text{La}_{1.8}\text{Sr}_{0.2}\text{NiO}_4$ [6].

These results have implications for two distinct cuprate systems. First of all, similar line shapes have been observed in superconducting $\text{YBa}_2\text{Cu}_3\text{O}_{6.6}$ [19]. There, the net width of the flat-topped peaks is smaller than in the nickelate case, implying wider antiferromagnetic domains. Nevertheless, the unusual shape suggests the presence of weakly correlated antiphase domains, as might be induced by fluctuating charge stripes. This analogy is important, because it suggests a uniform interpretation of the spin dynamics in the hole-doped cuprate systems studied so far with neutrons.

A second system to which a connection can be made is the electron-doped superconductor $\text{Nd}_{2-x}\text{Ce}_x\text{CuO}_4$. To see this, consider the measurements of the instantaneous correlation length, or its inverse, κ , that have been reported for $\text{Nd}_{1.85}\text{Ce}_{0.15}\text{CuO}_{4+\delta}$ [20] and $\text{La}_2\text{NiO}_{4.07}$ [14]. Such measurements involve an energy integration over the spin fluctuation cross section. In the paramagnetic phase of each of these systems, κ increases rapidly with temperature, differing substantially in each case from behavior of the undoped parent compound. The rapid variation of κ corresponds to the increase in Q width found in our inelastic measurements on the $\delta = 0.105$ crystal. The change in the temperature dependence of κ induced by doping has, in the former cases, been interpreted as evidence for a weakening of the effective superexchange, J , based on expectations for a 2D Heisenberg antiferromagnet. In contrast, our results for the $\delta = 0.105$ sample suggest that an analysis based on a spin-only

model is likely to be inadequate, and one should consider the effect of charge inhomogeneities. The similarity in the temperature and doping dependence of κ in the electron-doped cuprate and the nickelate suggests that one look for evidence of incipient charge stripes in as-grown $\text{Nd}_{1.85}\text{Ce}_{0.15}\text{CuO}_{4+\delta}$ at $T \gtrsim 200 \text{ K}$. Furthermore, the abrupt appearance of superconductivity for a Ce concentration $x \gtrsim 0.15$ might correspond to the stabilization of stripe correlations. Experimental tests are needed.

We gratefully acknowledge helpful discussions with V. J. Emery. Work at Brookhaven was carried out under Contract No. DE-AC02-76CH00016, Division of Materials Sciences, U.S. Department of Energy.

-
- [1] S. M. Hayden *et al.*, Phys. Rev. Lett. **68**, 1061 (1992).
 - [2] C. H. Chen, S.-W. Cheong, and A. S. Cooper, Phys. Rev. Lett. **71**, 2461 (1993).
 - [3] K. Yamada *et al.*, Physica C **221**, 355 (1994); K. Nakajima *et al.*, J. Phys. Soc. Jpn. **66**, 809 (1997).
 - [4] J. M. Tranquada, D. J. Buttrey, V. Sachan, and J. E. Lorenzo, Phys. Rev. Lett. **73**, 1003 (1994); J. M. Tranquada, J. E. Lorenzo, D. J. Buttrey, and V. Sachan, Phys. Rev. B **52**, 3581 (1995).
 - [5] P. Wochner, J. M. Tranquada, D. J. Buttrey, and V. Sachan, Report No. cond-mat/9706261; J. M. Tranquada, P. Wochner, A. R. Moodenbaugh, and D. J. Buttrey, Phys. Rev. B **55**, R6113 (1997).
 - [6] V. Sachan *et al.*, Phys. Rev. B **51**, 12742 (1995); J. M. Tranquada, D. J. Buttrey, and V. Sachan, Phys. Rev. B **54**, 12318 (1996).
 - [7] T. Ido, K. Magoshi, H. Eisaki, and S. Uchida, Phys. Rev. B **44**, 12094 (1991); X.-X. Bi and P. C. Eklund, Phys. Rev. Lett. **70**, 2625 (1993); D. A. Crandles, T. Timusk, J. D. Garret, and J. E. Greedan, Physica C **216**, 94 (1993); P. Calvani *et al.*, Phys. Rev. B **54**, R9592 (1996); T. Katsufuji *et al.*, Phys. Rev. B **54**, R14230 (1996).
 - [8] J. M. Tranquada *et al.*, Nature **375**, 561 (1995); J. M. Tranquada *et al.*, Phys. Rev. B **54**, 7489 (1996).
 - [9] J. M. Tranquada *et al.*, Phys. Rev. Lett. **78**, 338 (1997).
 - [10] S.-W. Cheong *et al.*, Phys. Rev. Lett. **67**, 1791 (1991) T. E. Mason, G. Aeppli, and H. A. Mook, Phys. Rev. Lett. **68**, 1414 (1992); T. R. Thurston *et al.*, Phys. Rev. B **46**, 9128 (1992); M. Matsuda *et al.*, Phys. Rev. B **49**, 6958 (1994); G. Aeppli, T. E. Mason, S. M. Hayden, and H. A. Mook, (preprint).
 - [11] G. Aeppli and D. J. Buttrey, Phys. Rev. Lett. **61**, 203 (1988); T. Freltoft *et al.*, Phys. Rev. B **44**, 5046 (1991).
 - [12] K. Yamada *et al.*, J. Phys. Soc. Jpn. **60**, 1197 (1991).
 - [13] K. Nakajima *et al.*, J. Phys. Soc. Jpn. **62**, 4438 (1993).
 - [14] K. Nakajima *et al.*, J. Phys. Soc. Jpn. **64**, 716 (1995).
 - [15] S. Hosoya *et al.*, Physica C **202**, 188 (1992).
 - [16] J. M. Tranquada *et al.*, Phys. Rev. B **50**, 6340 (1994).
 - [17] K. Nakajima *et al.*, Z. Phys. B **96**, 479 (1995).
 - [18] S. M. Hayden *et al.*, Phys. Rev. Lett. **76**, 1344 (1996).

- [19] B. J. Sternlieb *et al.*, Phys. Rev. B **50**, 12915 (1994); J. M. Tranquada *et al.*, Phys. Rev. B **46**, 5561 (1992).
 [20] M. Matsuda *et al.*, Phys. Rev. B **45**, 12548 (1992).

TABLE I. Summary of $\text{La}_2\text{NiO}_{4+\delta}$ samples, the nature of interstitial and magnetic order (C=commensurate, IC=incommensurate), magnetic-ordering temperature, and spin-wave velocity.

δ	Interstitial Order	Magnetic Order	T_m (K)	$\hbar c$ (meV-Å)
0.00		C	335	340
0.105	1D	C	55	70 ± 8
0.133	3D	IC	110.5	200 ± 20

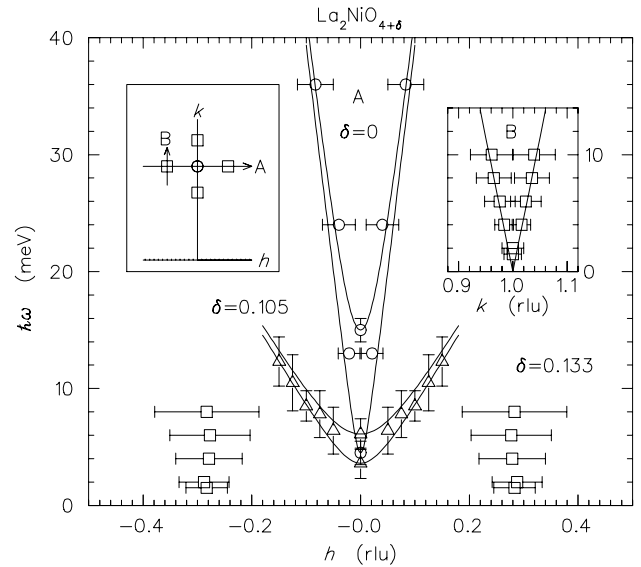


FIG. 1. Low-energy spin-wave dispersions measured on crystals of $\text{La}_2\text{NiO}_{4+\delta}$ with $\delta = 0$ (circles), 0.105 (triangles), and 0.133 (squares). Left inset indicates directions A and B in the $(h, k, 0)$ plane along which the dispersion has been characterized. Main panel shows dispersion along A ; results of scans along B for $\delta = 0.133$ are shown in the right inset. Bars indicate measured peak widths (except at $h = 0$ for $\delta = 0$), with no correction for resolution.

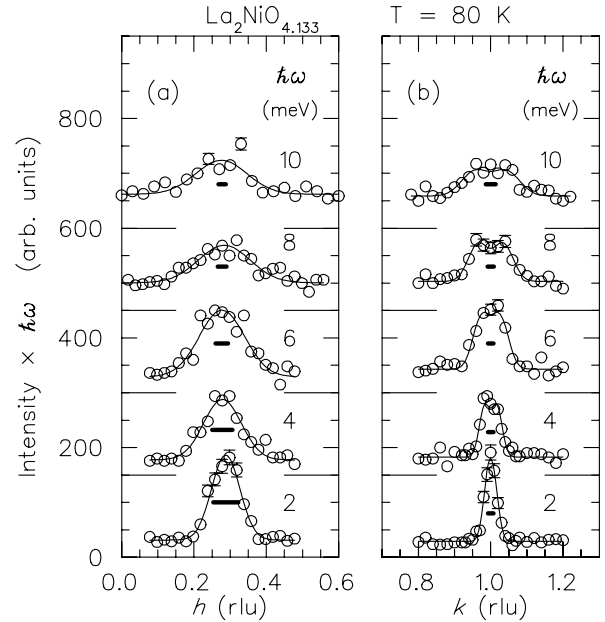


FIG. 2. Scans at constant energy transfer through the magnetic Bragg point $(0.278, 1, 0)$ of the $\delta = 0.133$ crystal at $T = 80$ K. (a) Type- A scans, as defined in Fig. 1. Lines through points are fits to a single Gaussian peak. (b) Type- B scans. Lines are fits of pairs of Gaussian peaks dispersing with energy as indicated by the line in the right inset of Fig. 1. Thick horizontal bars indicate calculated resolution width.

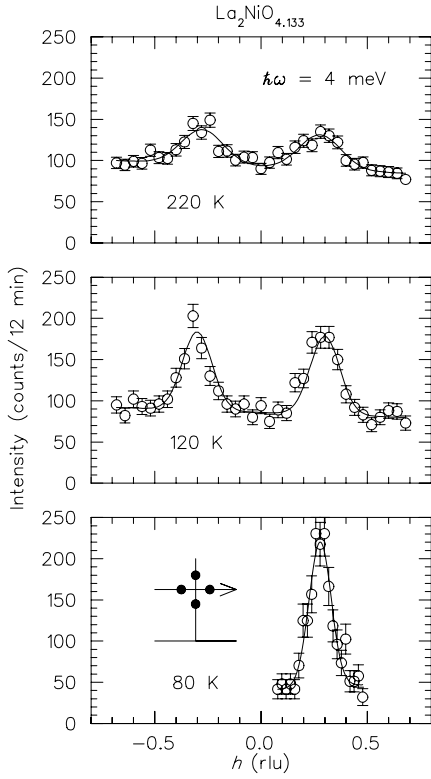


FIG. 3. Constant-energy scans at $\hbar\omega = 4$ meV through the incommensurate magnetic peak positions (as indicated in inset) at three temperatures: 80 K, 120 K and 220 K, the latter two being above the magnetic-order transition (110.5 K). The lines are fitted Gaussian peaks, symmetric about $h = 0$.

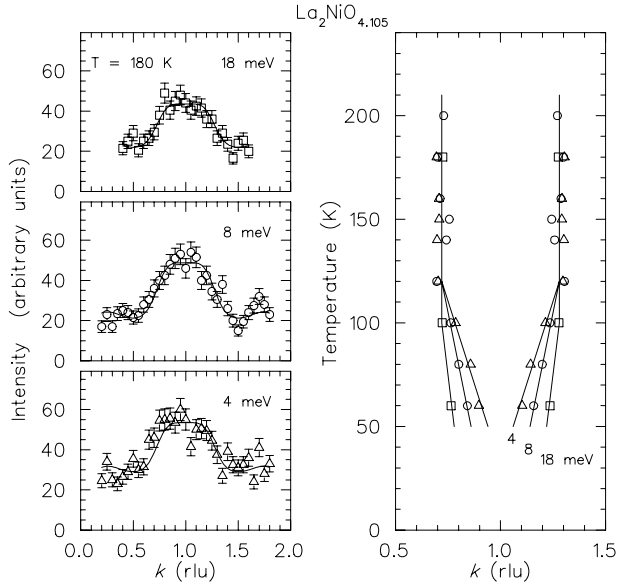


FIG. 4. Left: Constant-energy scans through the antiferromagnetic wavevector measured on the $\delta = 0.105$ crystal at $T = 180$ K ($\approx 3.6T_N$) with $\hbar\omega = 4, 8,$ and 18 meV. Lines are fits as described in the text. Right: Positions of half-maximum-intensity points (for peaks in constant- E scans) vs. temperature for $\hbar\omega = 4, 8,$ and 18 meV. Lines are guides to the eye.